Numerical study of fluid-structure interaction in supersonic regimes

Flat panel mouvement in a super-sonic fluid flow

Jérome Giordano – Yves Burtschell – Marc Medale
Pierre Perrier

Polytech Marseille
I.U.S.T.I UMR CNRS 6595
Technopôle de château Gombert
5, rue Enrico Fermi 13453 Marseille Cedex 13
Jerome.Giordano@polytech.univ-mrs.fr

ABSTRACT. *A numerical model of fluid-structure interaction has been developed. This numerical model allowed us to find the resonance phenomenon of the movement of an aluminium plate subjected to an eulerian supersonic flow on one of its faces. FFT of significant variables allow us to give an estimation of critical Mach number and pulsation, validated by an analytical model. Frequently neglected in the literature, an extension for the viscous fluid flow case is proposed. Thus, the plate movement amplification due to boundary layer detachment has been shown. An estimation of critical Mach number and pulsation has been given in this case, too.*

RÉSUMÉ. *Un modèle numérique d'interaction fluide-compressible-structure-élastique a été développé. Ce modèle numérique nous a permis de retrouver le phénomène de résonance du mouvement d'une plaque d'aluminium soumise à un écoulement supersonique eulerien sur une de ses faces. Via des FFT de variables caractéristiques, un encadrement du Mach et de la pulsation critique a été proposé et validé par rapport à un modèle analytique. Souvent négligée dans la littérature, une extension aux fluides visqueux est également proposée. Nous avons ainsi mis en évidence une amplification du mouvement de la plaque provoqué par les décollements de couche limite. Un encadrement du Mach et de la pulsation critique est également proposée dans ce cas.*

KEYWORDS: *fluid-structure interaction, flat panel, Navier-Stokes.*

MOTS-CLÉS : *interaction fluide-structure, plaque plane, Navier-Stokes.*

1. Introduction

The purpose of this paper is the numerical study of fluid-structure interaction phenomena in compressible flows. Indeed, structure vibrations may induce boundary layer detachments, cause structure damages and significantly modify the fluid flow (such as the location and the configuration of shock waves). This kind of problem may occur at the atmospheric spacecraft re-entries, in presence of strong vibration of planes wings or tail and more particularly on supersonic flights and on bending of rocket nozzle, etc.

Although the study of these issues has already been treated with analytical models (for example in [BIS 55] and [FUN 55]), but in a rather approximate way, the advent of computational methods, in structural analyses as well as in fluid flows, allows a new approach on the subject. Thus problems are studied more precisely by a better description of the geometry domain as can be shown on the completely simulation of a full F-16 on flight realized by Geuzaine *et al.* [GEU 01] or by using more sophisticated physical models. In this way, taking into account the viscosity effects may be a next step, more particularly in hyper-sonic flow. Indeed, with these flow cases, only a Navier-Stokes (NS) modeling may simulate all shock waves configurations, as Burtschell has shown in [BUR 02]. One can note that in transonic case there are more study which have been achieved, particularly by Gordnier in [GOR 01].

In this article, we present the result of a NS modeling for the study of the 2D movement of a flat panel in super-sonic flow, compared to inviscid flow. Dealing with this problematic, Bisplinghoff *et al.* [BIS 55] proposed an analytical model which describes the movement of the panel in the case of inviscid flow. This model gives an estimation of the critical Mach number and critical frequency and commonly serves as a reference to validate the numerical codes of fluid structure interaction. Thus, Farhat and co-workers used this model to validate their numerical models in [FAR 95], [FAR 96], [PIP 97] and [PIP 00]. Furthermore, the validation of the numerical approach of Lefrancois *et al.* is based on the critical Mach number determination [LEF 98] and [LEF 00]. These references establish this problematics to be a test case in an inviscid flow case.

Our numerical model is based on the coupling of two heterogeneous codes: a finite volume code which describes reactive transient NS flows and a finite element code which describes the structure dynamics. The coupling is carried out by the means of a serial algorithm. This numerical strategy is frequently used and one can have an overview of its application by the reading of [FEL 01].

After describing the various physical models and their corresponding numerical counterparts, we shall present our approach in order to deal with the fluid-structure interaction problems. A validation is presented in the case of inviscid fluid flow and an extension is proposed in the case of viscous flow. We shall discuss the result in both cases and we shall conclude.

2. Description of constitutive models

We present the different physical models and then we expose a brief description of numerical models associated to each domain.

2.1. *Physical models describing hyper-enthalpic fluid flows*

We consider the following assumptions related to the fluid flow domain:

– the fluid is a continuous medium;

– its rheological behavior is Newtonian;

– it is compressible;

– gravity is neglected;

– the flow is laminar;

– it is a mixture of N_s perfect gases.

The different conservation laws are:

– mass equation:

$$\frac{\partial \rho_{es}}{\partial t} + \frac{\partial \rho_{es} u_{es\,i}}{\partial x_i} = \omega_{es} \qquad [1]$$

in which x_i is the cartesian coordinate in the i direction, t the time, ρ_{es} the density of the species es, $u_{es\,i}$ the velocity of the species in the i space direction and ω_{es} its production rate due to chemical reactions. In this article, frozen cases are considered thus ω_{es} is equal to zero.

– momentum equation:

$$\frac{\partial \rho u_j}{\partial t} + \frac{\partial \left(\rho u_j u_i + p\delta_{ij} - \tau_{ij}\right)}{\partial x_i} = 0 \qquad [2]$$

in which p is the mixture pressure, τ_{ij} the tensor of shear stresses and δij the Kronecker symbol;

– energy equation:

$$\frac{\partial \rho e}{\partial t} + \frac{\partial \left(\rho u_i e + u_i p - u_i \tau_{ij} + q_i\right)}{\partial x_i} = 0 \qquad [3]$$

in which e is the energy and q_i the heat flow in the direction i.

2.2. *Numerical models for hyper-enthalpic flows simulation*

2.2.1. *Fixed grid case*

In the previous section we have given Navier-Stokes's equations governing the fluid domain for a N_s mixture of perfect reactive gases. This equations set can also be written as following

$$\frac{\partial \mathbf{U}}{\partial t} + div\left[\mathcal{F}(\mathbf{U})\right] = \mathbf{\Omega}^c \quad [4]$$

with

– $\mathbf{U}$ is the conservative variables vector:

$$\mathbf{U} = \left(\rho Y_1, ..., \rho Y_{N_s}, \rho u, \rho v, \rho w, \rho e\right)^T \quad [5]$$

– $\mathbf{\Omega}^c$ is the chemical source term:

$$\mathbf{\Omega}^c = \left(\omega_1, ..., \omega_{N_{sc}}, 0, ..., 0\right)^T \quad [6]$$

for frozen gazes $\mathbf{\Omega}^c = \overrightarrow{0}$

– $\overrightarrow{\mathcal{F}}(\mathbf{U})$ is the sum of the fluxes vector in the 2 space directions which may be decomposed by a diffusive part and a convective part, for example in the direction $\overrightarrow{e_x}$: $F\overrightarrow{e_x} = \left(F_c + F_d\right)\overrightarrow{e_x}$

A discretization of these equations by a finite volume method enables to get the following form:

$$\frac{\partial \mathbf{U}_i}{\partial t}\int_{C_i} d\mathcal{V} + \sum_{k=1}^{faces}\left(\left(\overrightarrow{\mathcal{F}_k}\right)\int_{\partial C_i^k}\overrightarrow{n}\, d\mathcal{S}\right) = \mathbf{\Omega}_i^c\int_{C_i} d\mathcal{V} \quad [7]$$

The solution of this set of equation is made by a second order scheme, both in space and time. For this study a Van-Leer slope limiter has been used.

Moreover, we distinguish the calculation of the convective fluxes from the diffusive ones. Convective fluxes are calculated by the solution of a Riemann problem on each interfaces. This solution may be performed by an exact solver or an approached one (HLLE, HLLC, ROE, AUSM, etc.). For its accuracy and efficiency solution a HLLC solver has been used. Diffusive fluxes are estimated by the means of a finite differences method. Toro, [TOR 97], deals with a complete review of these problems.

2.2.2. *Moving grid case*

In the case of a fluid-structure interaction problem, the domain of fluid may change with the time, and so may the mesh. A eulerian kinematics description may induce significant errors, which may compel us to use an *Arbitrary Lagrangian Eulerian* description. So the equation [7] becomes:

$$\frac{\partial}{\partial t}\left(\mathbf{U}_i\int_{C_i} d\mathcal{V}(t)\right) + \sum_{k=1}^{faces}\left(\left(\overrightarrow{\mathcal{F}_k} - \overrightarrow{w_k}\mathbf{U}_k\right)\int_{\partial C_i^k}\overrightarrow{n}\, d\mathcal{S}\right) = \mathbf{\Omega}_i^c\int_{C_i} d\mathcal{V}(t) \quad [8]$$

in which $\overrightarrow{w_k}$ is the velocity vector of cell frontiers.

2.3. *Error induced with a purely eulerian formulation*

Although a non-ALE modeling of the fluid flow, in the case of moving domain, is theoretically wrong, we wanted to estimate the error generated by this simplification. Our purpose is to know if this simplification can be made; if so, we will obtain a faster simulation.

To quantify this error, we have simulated the evolution of the fluid flow in a $1D$ shock tube of the test case of Sod [SOD 78], for a fixed and a moving grid with non-ALE and ALE description. The velocity of the cells are imposed as described on the figure 1

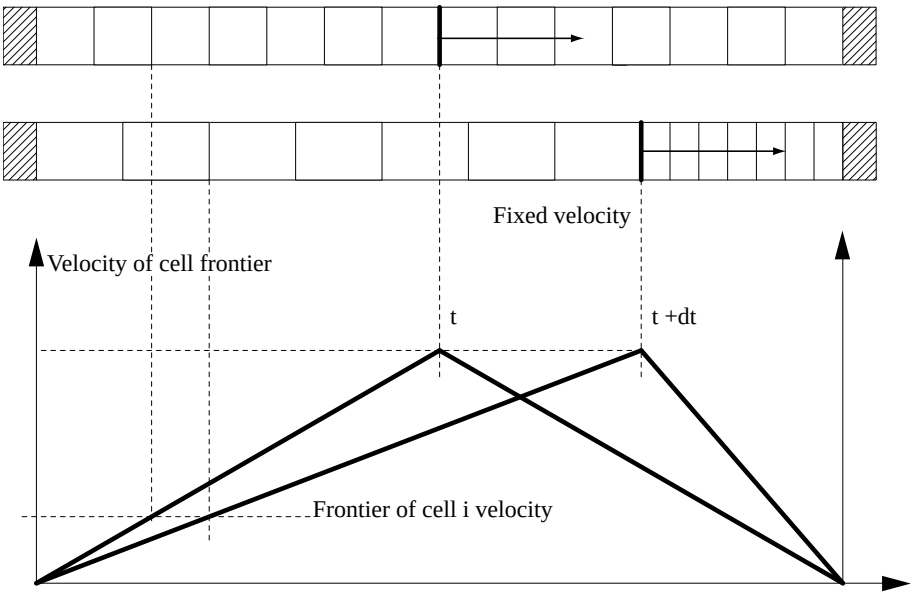

Figure 1. *Velocity of cells*

The maximum of the velocity is imposed at $100\ m/s$, $20\ m/s$, $10\ m/s$.

We have compared the evolution of the physical velocity and density of fluid at time $t = 55\ ms$, given by a HLLC solver for the three cases: fixed domain, moving domain with non-ALE description and moving domain with ALE description.

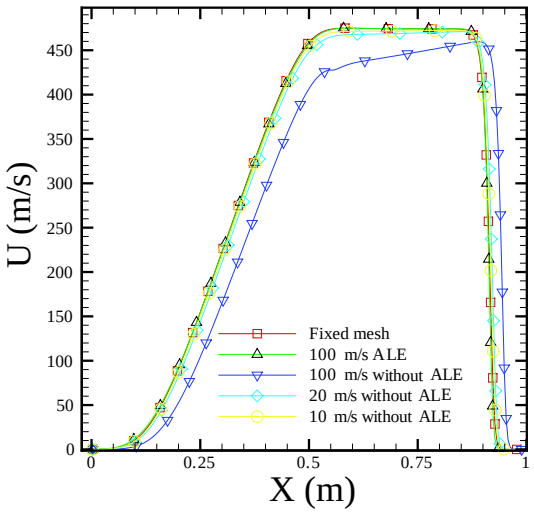

Figure 2. *Velocity profile*

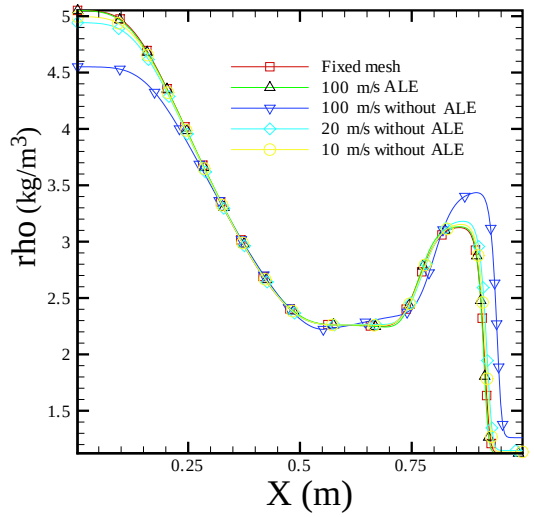

Figure 3. *Density profile*

We may conclude that for low cells velocity a non-ALE description does not generate large disturbances. The extension of this conclusion to the multidimensional cases may be discussed. Indeed if the fluid flow has a particular space direction and the mesh is moving into another direction, the cells velocity will be of the same order

as the physical fluid velocity. In this case the disturbance of a non-ALE description is more difficult to estimate.

2.4. *Physical models describing the structural dynamics*

We use the following assumptions for this domain:

– the solid is considered as isotropic and homogeneous;

– the gravity is neglected;

– the structure remains in small strains and in its elastic domain (linear range);

– we consider no material-damping.

According to these hypotheses, the strain tensor $\overline{\overline{\varepsilon}}$ is defined by:

$$\overline{\overline{\varepsilon}} = \frac{1}{2}\left(\overline{\overline{grad}}\xi(M,t) + \overline{\overline{grad^t}}\xi(M,t)\right) \quad [9]$$

with $\overrightarrow{\xi(M,t)}$ the displacement vector of M at the moment t.

– The behaviour law is the Hooke's relation for the multidimensional cases:

$$\overline{\overline{\sigma}}(M,t) = \mathcal{H}\overline{\overline{\varepsilon}}(M,t) + \overline{\overline{\sigma}}_0 \quad [10]$$

with $\overline{\overline{\sigma}}$ is the strain tensor and $\mathcal{H}$ the Hooke's tensor.

– The local equation of the structural dynamics is:

$$\overrightarrow{div}\overline{\overline{\sigma}}(M,t) + \overrightarrow{f_v} = \rho_s \frac{\partial^2 \xi(M,t)}{\partial t^2} \quad [11]$$

with $\overrightarrow{f_v}$ the body forces and ρ_s the material density.

To this equation, two boundary conditions are associated

– kinematic type:

$$\overrightarrow{\xi}(\forall M \in \partial_1 S, t) = \overrightarrow{\xi_d} \quad [12]$$

with $\partial_1 S$ the part of structure boundary S where displacement $\overrightarrow{\xi_d}$ are imposed;

– stress type:

$$\overline{\overline{\sigma}}(\forall M \in \partial_2 S, t) \circ \overrightarrow{n} = \overrightarrow{F_d} \quad [13]$$

with $\partial_2 S$ the part of structure boundary S where stress $\overrightarrow{F_d}$ are imposed and $\overrightarrow{n}$ the outward normal at the considered point.

2.5. *Numerical model of structural dynamics*

We use a finite element method to discretize this equation in space, whereas the temporal time integration is achieved with the Newmark's algorithms which leads to the following discretized equation

$$(\mathbf{M} + \gamma\Delta t\mathbf{C} + \beta\Delta t^2\mathbf{K})\ddot{x}_{n+1} = \mathbf{F}_{n+1} - \mathbf{C}\tilde{\dot{x}}_{n+1} + \mathbf{K}\tilde{x}_{n+1} \quad [14]$$

$$\tilde{\dot{x}}_{n+1} = \dot{x}_n + (1-\gamma)\Delta t\ddot{x}_n \quad [15]$$

$$\tilde{x}_{n+1} = x_n + \Delta t\dot{x}_n + \frac{\Delta t^2}{2}(1-2\beta)\ddot{x}_n \quad [16]$$

$\mathbf{M}$ is the mass matrix, $\mathbf{C}$ the damping matrix (which is equal to zero if the structural damping is neglected), $\mathbf{K}$ the stiffness matrix. These matrix are the result of space finite element discretization of the equation 11. This discretization is performed by a quadrangle with four nodes (C_0 class and bi-linear [BAT]) .

The acceleration, velocity and location of the vector variables at the time $(t = t_n)$ are respectively: $\ddot{x}_n,\ \dot{x}_n,\ x_n$. The parameters β and γ determine the stability and the accuracy characteristics of the algorithm under consideration. Stability is achieved for $\frac{1}{2} \leq \gamma \leq 2\beta$ and in this study the first scheme of table 1 is used. Numerical properties of some classical methods are summarized in the table 1 [HUG 87].

Method	Type	β	γ	Order of accuracy
Average acceleration (trapezoidal rule)	Implicit	$\frac{1}{4}$	$\frac{1}{2}$	2
Linear acceleration	Implicit	$\frac{1}{6}$	$\frac{1}{2}$	2
Fox-Goodwin (royal road)	Implicit	$\frac{1}{12}$	$\frac{1}{2}$	2
Central difference	Explicit	0	$\frac{1}{2}$	2

Table 1. *The Newmark family*

3. Numerical strategy of coupling

The numerical coupling between the fluid flow and the structural dynamics models is performed through boundary conditions. The fluid flow imposes a pressure distribution on the structure boundary which in return imposes a new geometry to the fluid domain. Communications between the two codes result in a staggered serial algorithm as described on figure 4.

For the load and motion transfer a matching interface is used as it is shown on the figure 5.

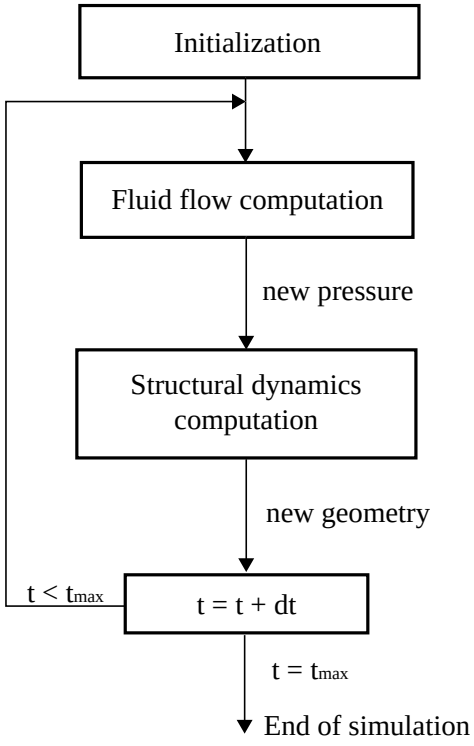

Figure 4. *Coupling algorithm*

If the viscosity is neglected in the terms of loading, fluid flow pressure loads the structure along the interface as follows:

$$\overline{\overline{\sigma}}(\forall M \in \partial_2 S, t) \circ \overrightarrow{n} = -p \circ \overrightarrow{n} \quad [17]$$

$$\overline{\overline{\sigma}}(\forall M \in \partial_2 S, t) \circ \overrightarrow{t} = \overrightarrow{0} \quad [18]$$

The structure, in return, imposes a velocity to the interface nodes. For non-matching interfaces, interpolation methods have been developed in [FAR 98].

3.1. *Description of the study case*

We consider a clamped flat aluminium panel whose dimensions are: length $L = 500\ mm$ and thickness $h = 1.35\ mm$ of unit width. One of its faces is subjected to a supersonic fluid flow, characterized by the inlet conditions: the pressure

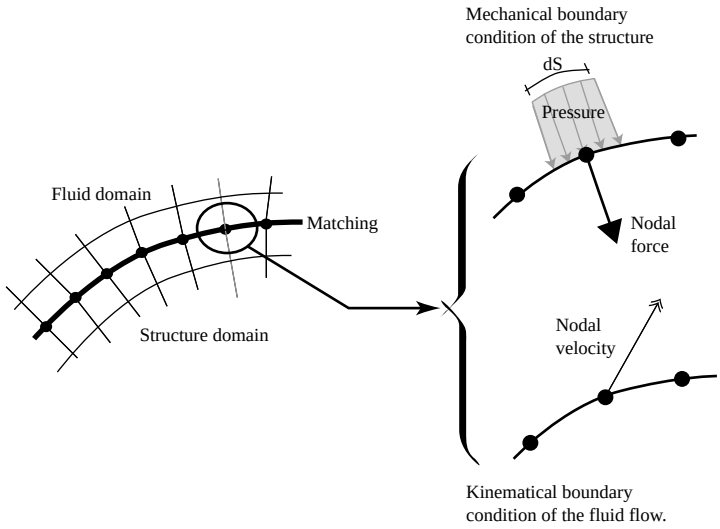

Figure 5. *Load and motion transfer at the fluid structure interface*

P_∞, the density $\rho_\infty = 0.4$ and the Mach number $Mach_\infty$. On the other face there is a motionless fluid domain at the constant pressure $P_\infty = 13000\ Pa$. The modeling is made in 2 dimensions and we will describe the movement of the flat panel for different Mach number ranging from 1.3 et 2.8 to find the critical Mach number and critical circular frequency which lead to the unstable aeroelastic mode.

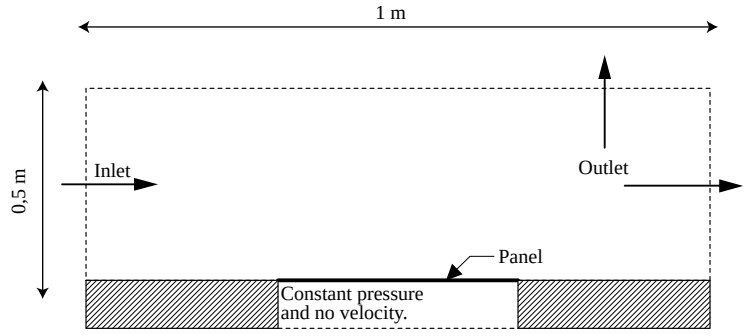

Figure 6. *Geometry of the problem*

In the case of inviscid fluid flow, the analytical model proposed by R. L. Bisplinghoff [BIS 55] allows a description of the movement of the panel. The left hand

side of [19] is the equation of the free movement of a plate and the right one is the modeling of the pressure, so we have

$$\rho_s h \frac{\partial^2 w(x)}{\partial t^2} + \frac{Eh^3}{12(1-\nu^2)} \frac{\partial^4 w(x)}{\partial x^4} = -\frac{\rho_\infty u_\infty^2}{\sqrt{M_\infty^2 - 1}} \frac{\partial w(x)}{\partial x} - \frac{\rho_\infty u_\infty (M_\infty^2 - 2)}{(M_\infty^2 - 1)^{\frac{3}{2}}} \frac{\partial w(x)}{\partial x} \quad [19]$$

In which $\rho_s = 2710\ kg.m^{-3}$, $E = 77.28\ GPa$. The model evaluates the critical Mach number at $Mach_{critical} = 2.1$ and the circular frequency at $\omega_{critical} = 460\ rad.s^{-1}$.

3.2. *description of the meshes and the time step used*

Two meshes have been used for the fluid flow problem: one for the inviscid case (M_1) and another one for the viscous case (M_2). M_1 is made up of 200×100 equal spacing nodes. For the viscous fluid flow case, the same nodes number has been used, but the dimension of the wall cell is fixed at $1.\ 10^{-5}\ m$ and ratio of the first and last cell is $\frac{C_1}{C_{100}} = 2.\ 10^{-3}$ in order to capture the boundary layer. The structure mesh in the panel is constituted of 100×1.

For the determination of the time step, one can note that various types of algorithms were studied by C. Farhat et S. Piperno [PIP 97] and they have explained the different problems induced by large time steps (problems of energy conservation, etc.). We present the convergence of the period value function of the coupling step on the fig 8.

In this article we have chosen to use small time step with respect of fluid structure dynamics ($\approx \frac{Period}{100} \approx 10^{-4}\ s$) to preserve conservative couplings. The Geometric Conservation law is checked with small time steps, as it is shown by Lesoinne in [LES 95].

We are only focusing on the established periodic mode of the phenomenon: we do not consider the transient response of the flat panel to a shock wave passage. So, owing to this consideration, the panel is initially deformed and we are waiting for a converged fluid flow on this geometry. This is the first step of the numerical simulation of the fluid structure interaction problem. From this configuration, the structure is free and the flow imposed by the inlet conditions.

4. Results

4.1. *Inviscid flow case*

To determine the velocity of the fluid flow which leads to the unstable aeroelastic mode, we have compared the evolution of three parameters: the lift C_p and the displacement of two points, the first one at $0.25\ m$, the middle of the flat panel, and the

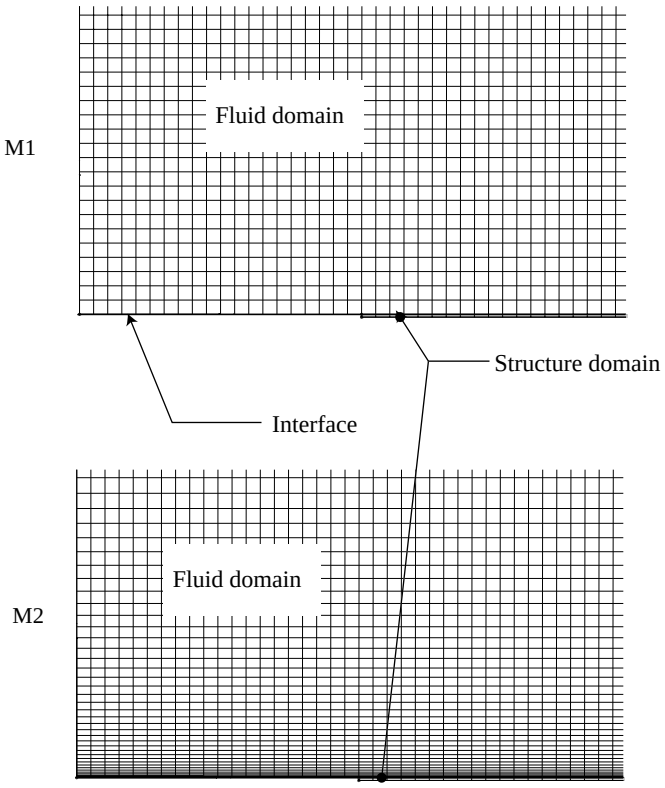

Figure 7. *Zoomed mesh for fluid flow*

second one at $0.35\ m$. A Fast Fourier Transform (FFT) of the time series associated with each variable allows an optimal reading of results. In a first time, we have explored a large range of fluid flow velocity, included between Mach 1.3 and Mach 2.8 but on short exploration time $\approx 0.1\ s$. We observe that the period of the panel movement is always included between $[\ 0.0135\ s\ ;\ 0.0140\ s\ ]$, it corresponds to circular frequency included in $[\ 449\ rad.s^{-1}\ ;\ 465\ rad.s^{-1}\ ]$. We also see that the evolution of the lift is not a real sinusoid, as it is shown on the figure 9.

To explain this evolution, we have superposed the position of the flat panel on the curve of the lift during one period (fig. 10).

So we can say that:

– the C_p increases when:

- the panel is inside the fluid domain and is going far from it;
- the panel is outside the fluid domain and is going towards it.

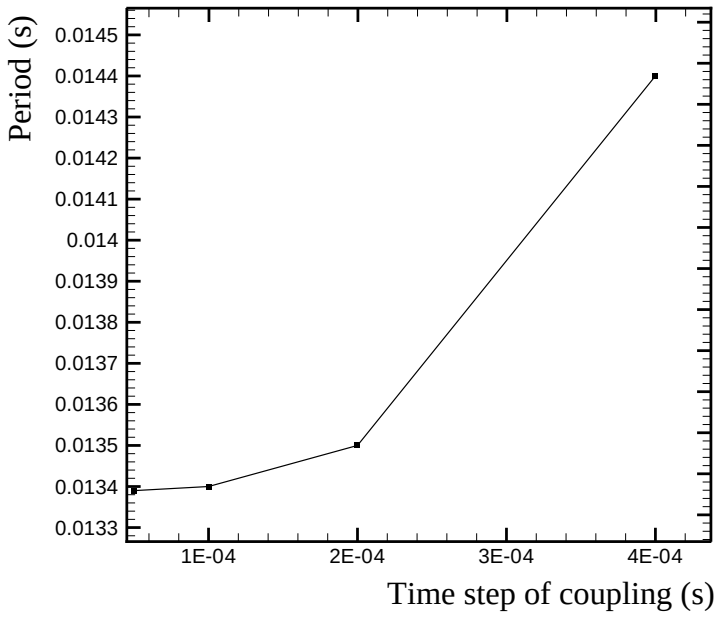

Figure 8. *Period convergence for differents coupling steps*

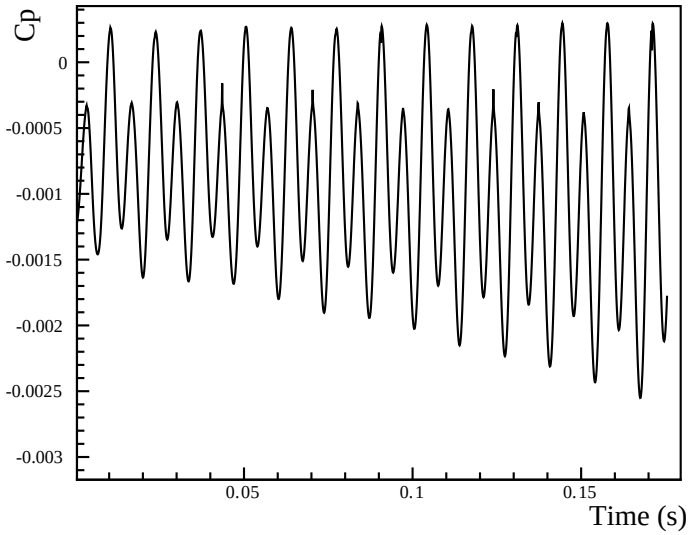

Figure 9. *Time evolution of the lift coefficient*

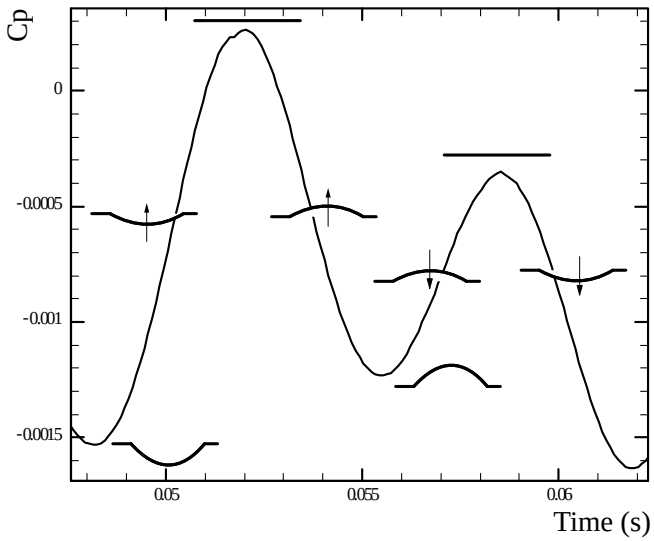

Figure 10. *time evolution of the lift coefficient and corresponding movement of the panel during one period*

– Conversely the C_p decreases when:

- the panel is outside the fluid domain and is going far from it;
- the panel is inside the fluid domain and is going towards it.

This description is available in the case of a flat panel on the top of fluid domain. We verify also that the C_p is lower when the deformation is weak, but the structure convexity does not modify the sign of the lift.

The FFT of each time series allows to find the characteristic frequency of the phenomenon. Thus, we can see the primary frequency f_p, which is included in $[\ 71\ Hz\ ;\ 74\ Hz\ ]$ and its higher orders: $2f_p$, $3f_p$...

On the figure 12 are represented the FFT of the C_p at the fourth order for different inlet fluid flow velocities and for a time exploration of $0.09\ s$.

Considering the magnitude and the width of the plots, we can say that configurations belonging to the $[2.2\ ;\ 2.3]$ range are closer to the unstable aeroelastic mode than the other ones. Now, we perform more detailed computations only for these Mach number, for a longer exploration time.

On the figure 13 are represented the FFT of C_p for an exploration time of $0.6\ s$. This new simulation allows us to estimate more precisely the most unstable mode, indeed Mach 2.1 and 2.3 curves are opened whereas the curve of Mach 2.2 does not. Thus, the unstable mode may be estimated close to Mach 2.2, it is corresponding to a

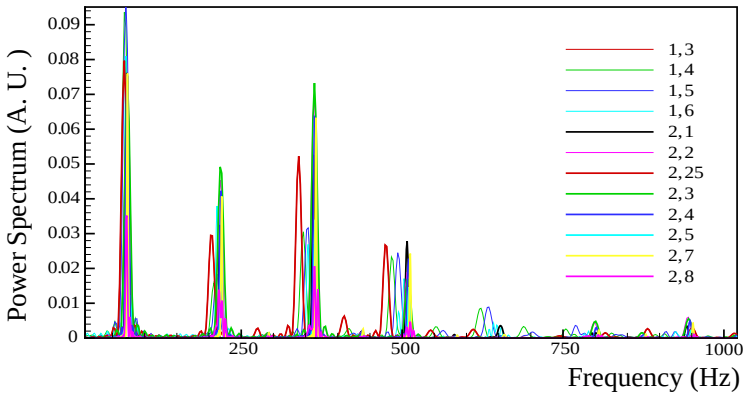

Figure 11. *FFT of the displacement at* $x = 0.35$ *m*

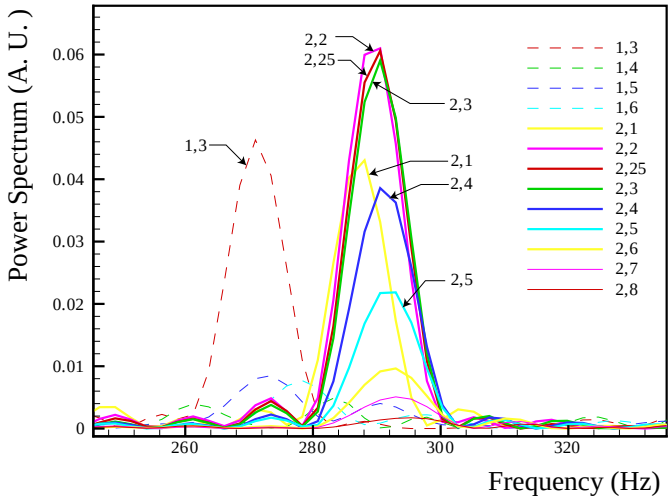

Figure 12. *FFT of* C_p *at* $4f_p$*, eulerian modeling,* 0.09 s *time of exploration*

circular frequency of $\omega_{critical} \approx 455\ rad.s^{-1}$. This result is in good agreement with the analytical model [19] and confirmed by a deviation of about 1% of the circular frequency.

4.2. *Viscous flow case*

In this part, the viscosity is taken into account, and the boundary layer detachment as a consequence. These phenomena appear in expansion zones as represented on

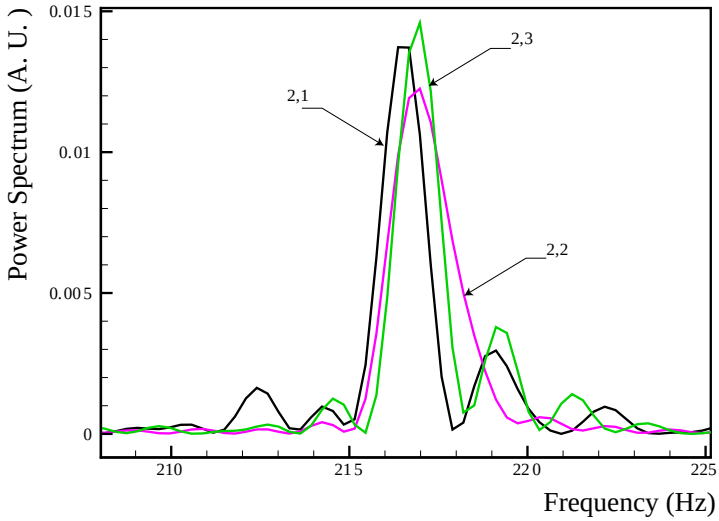

Figure 13. *FFT of C_p at $3f_p$, eulerian modeling, 0.6 s time of exploration*

figure 14. To have a good view of the boundary layer detachment, the Y scale is magnified by a factor 10, the maximal deviation of the plate, about 2 cm, respects the small strain assumption.

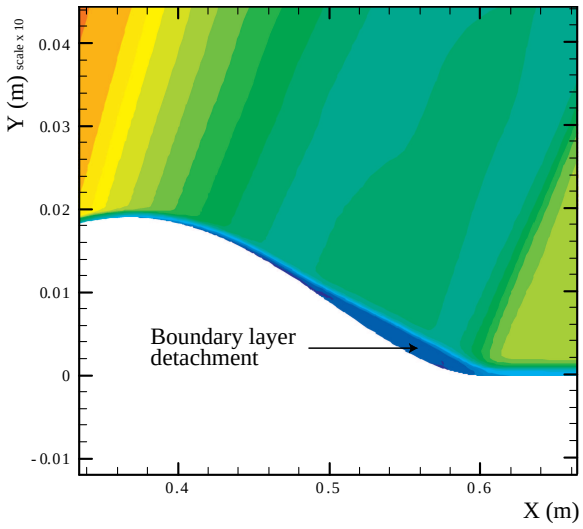

Figure 14. *Iso-value of the density, boundary layer detachment*

This boundary layer detachment induces an increase of the pressure by a modification of the expansion zone as represented on figure 15. This detachment plays the role of a fictitious wall for the fluid flow.

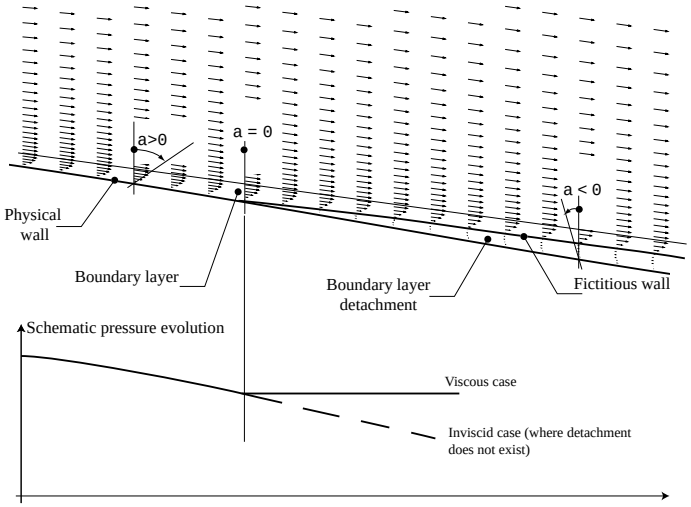

Figure 15. *Pressure evolution along the expansion zone*

Thus, in NS fluid flow the pressure is more important than in the eulerian case and the structure acceleration as a consequence. For the same reason the magnitude of C_p is greater in NS case than in the eulerian one the figure 16.

These consequences are very important, although we may have thought that the viscosity induces dissipative effects, there is an increase in the magnitude of the movement of the flat panel. So, even if in this study case the consequences on structure damages are not considered, taking into account the viscosity is essential to study the fluid-structure interactions problems, since the interaction takes place in the fluid flow boundary layers.

For this viscous case, we have also estimated the unstable mode. On the figure 17 are represented the ninth order FFT of the displacement at point at 0.35 m for an exploration time of $0.45\ s$. Through the comparison to the magnitude and the width of curves, we may estimate the unstable mode to be included between Mach 2.2 and 2.3. While the C_p magnitude significantly differs between NS than Euler configuration, the circular frequency is quite unchanged. The value of the critical circular frequency is $\omega_{critical} \approx 457\ rad.s^{-1}$, less than 1% of variation compared to the eulerian result.

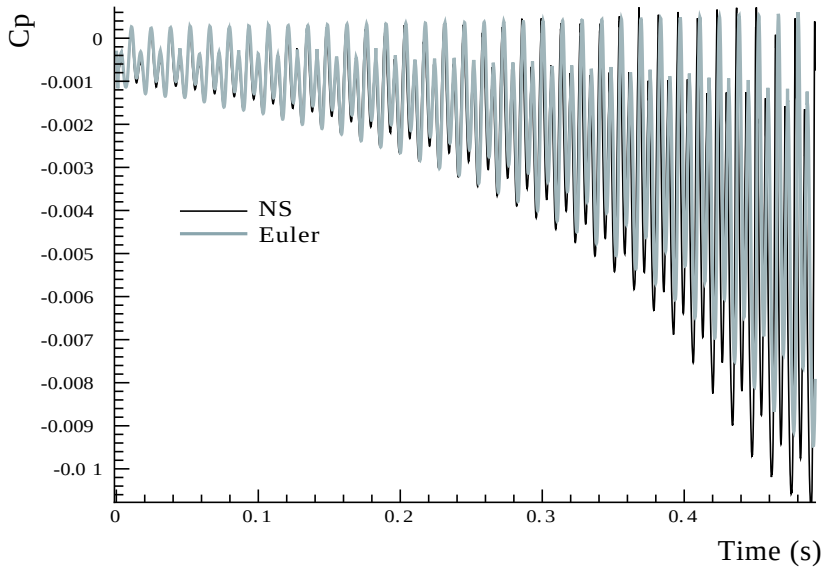

Figure 16. *Lift comparison between inviscid and viscous case*

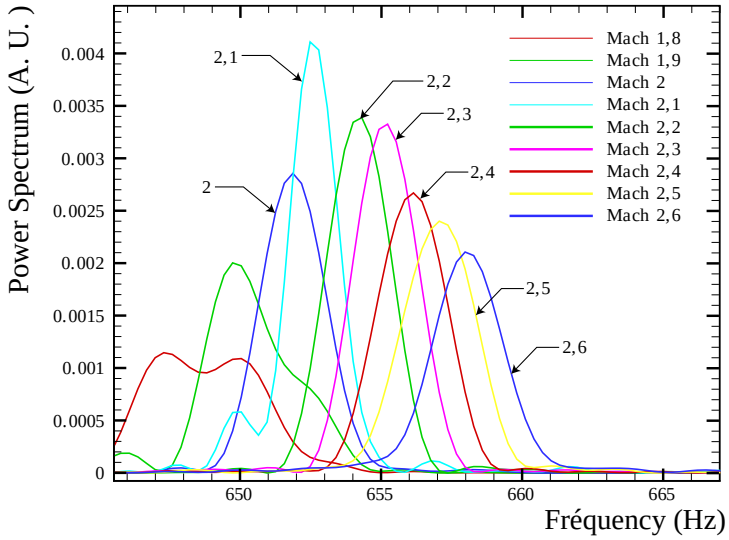

Figure 17. *FFT of the displacement at point at* 0.35 *m at the ninth order,* 0.45 s *time of exploration*

5. Conclusion

This study deals with the modeling of fluid-structure interaction in the case of the movement of a flat panel in a supersonic fluid flow. A numerical model, based on the coupling of two heterogeneous codes, was developed and allows us to study the unstable aeroelastic mode. In the case of inviscid fluid flow, we have compared our computed critical Mach number and circular frequency to those provided by an analytical model: $Mach_{critique} \approx 2.2$ et $\omega_{critical} \approx 455\ rad.s^{-1}$. After validating our approach in the eulerian case, we have extended the study to the viscous case. Taking into account of viscosity induces an amplification of the movement of the panel. This amplification arises owing to the higher pressure gradient in the boundary layer detachment. In this viscous case we have also estimated the critical Mach number and the critical circular frequency: $Mach_{critical} \in [2.2\ ;\ 2.3]$ et $\omega_{critical} \approx 457\ rad.s^{-1}$. This study was a first step in our more global approach which aims to deal with more complex fluid-structure interaction taking place in hyper-enthalpic fluid flows.

6. References

[BAT] BATOZ J.-L., DHATT G., *Modélisation des structures par éléments finis*, Hermes.

[BIS 55] BISPLINGHOFF R. L., ASHLEY H., HALFMAN R. L., *Aeroelasticity*, Dover books on physics, 1955.

[BUR 02] BURTSCHELL Y., ZEITOUN D. E., "Shock wave interactions in an axisymmetric steady flow", *Shock Waves*, , 2002.

[FAR 95] FARHAT C., LESOINNE M., MAMAN N., "Mixed explicit/implicit time integration of coupled aeroelastic problem : three field formulation, geometrical conservation and distributed solution", *International Journal of Numerical Methods in Fluids*, vol. 21, 1995, p. 807-835.

[FAR 96] FARHAT C., "High performance simulation of coupled nonlinear transcient aeroelastic problem", *Actes de la 3e école d'été de modélisation numérique en thermique*, Ile de Porquerolles, Juillet 1996, p. C6 1-79.

[FAR 98] FARHAT C., LESOINNE M., TALLEC P. L., "Load and motion transfer algorithms for fluid-structure interaction problems with non-matching discrete interfaces: momentum and energy conservation, optimal discretization aeroelasticity.", *Computer Methods in applied mechanics and engineering*, vol. 157, 1998, p. 95-114.

[FEL 01] FELIPPA C. A., PARK K. C., FARHAT C., "Partitioned analysis of coupled mechanical systems", *Computer Methods in applied mechanics and engineering*, vol. 190, 2001, p. 3247-3270.

[FUN 55] FUNG Y. C., *An Introduction to the theory of Aeroelasticity*, Wiley, 1955.

[GEU 01] GEUZAINE P., BRAOWN G., FARHAT C., "Aeroelastic dynamic analysis of a full F-16 configuration for various flight conditions", *AIAA Journal*, vol. 41, num. 3, March 2001, p. 363-371.

[GOR 01] GORDNIER R. E., VISBAL M. R., "Development of a three-dimensional viscous aeroelastic solver for nonlinear panel flutter", *Journal of fluids and structures*, vol. 16, num. 4, August 2001, p. 497-527.

[HUG 87] HUGHES T. J., *The finite element method. Linear static and dynamic finite element analysis*, Prentice-Hall, Englewood Cliffs, New Jersey, 1987.

[LEF 98] LEFRANÇOIS E., DHATT G., VANDROMME D., "Modèles numériques de couplage fluide-structure", *Actes de la 4e école d'été de modélisation numérique en thermique*, Ile de Porquerolles, Juillet 1998, p. C2 57-88.

[LEF 00] LEFRANÇOIS E., DHATT G., VANDROMME D., "Numerical study of the aeroelastic stability of an overexpanded rocket nozzle", *Revue européenne des élément finis*, vol. 9, num. 6-7, 2000, p. 727-762.

[LES 95] LESOINNE M., FARHAT C., "Geometric conservation laws for flow problems with moving boundaries and deformable meshes, and their impact on aeroelastic computations", *Computer Methods in applied mechanics and engineering*, vol. 134, 1995, p. 71-90.

[PIP 97] PIPERNO S., FARHAT C., "Design and evaluation of staggered partionned procedures for fluid-structure interaction simulations", *Rapport de Recherche 3241 INRIA*, , 1997.

[PIP 00] PIPERNO S., FARHAT C., "Design of efficient partitioned procedures for the transient solution of aeroelastic problems", *Revue européenne des élément finis*, vol. 9, num. 6-7, 2000, p. 655-680.

[SOD 78] SOD G., "A survey of several finite difference method for systems of nonlinear hyperbolic conservation laws.", *J Comput Phys*, vol. 27, 1978, p. 1-31.

[TOR 97] TORO E. F., *Riemann solvers and numerical methods for fluid dynamics*, Springer, 1997.